Electrochimica Acta 174 (2015) 640–646

Contents lists available at ScienceDirect

Electrochimica Acta

journal homepage: www.elsevier.com/locate/electacta

Study of the potentiometric properties of spinel-type manganese oxide doped with gallium and anions $Ga_{0.02}Mn_{1.98}O_{3.98}X_{0.02}$ ($X = S^{2-}$ and F^{-}) as selective sensor for lithium ion

Diego N. David-Parra[a], Nerilso Bocchi[b], Marcos F. S. Teixeira[a,*]

[a] Faculty of Science and Technology, São Paulo State University (UNESP), Presidente Prudente, SP - Brazil
[b] Department of Chemistry, Federal University of Sao Carlos, Sao Carlos, SP - Brazil

ARTICLE INFO

Article history:
Received 29 April 2015
Received in revised form 28 May 2015
Accepted 29 May 2015
Available online 4 June 2015

Keywords:
potentiometric behaviour
selective sensor
lithium ion
spinel-type manganese oxide
anionic doping

ABSTRACT

This paper describes the development of a selective lithium ion sensor based on spinel-type manganese oxide doped with gallium and anions ($Ga_{0.02}Mn_{1.98}O_{3.98}X_{0.02}$, where $X = S^{2-}$ and F^{-}). Investigation was made of the influence of cationic and/or anionic doping agents on the potentiometric response of the sensor. Experimental parameters evaluated included the effect of the lithium concentration on activation of the sensor by cyclic voltammetry, the pH of the electrolyte solution, and the selectivity towards Li^{+} compared to other alkali and alkaline-earth metal ions. There was an important influence of the unit cell size of the material on the linear range, detection limit, and selectivity of the sensor. Reduction in the size of the tunnel for insertion of the lithium in the porous structure of the oxide directly affected the potentiometric performance of the electrode. Sensor performance increased in the order: $Ga_{0.02}Mn_{1.98}O_4 > Ga_{0.02}Mn_{1.98}O_{3.98}S_{0.02} > Ga_{0.02}Mn_{1.98}O_{3.98}F_{0.02}$. The observed super-Nernstian response could be explained by a mixed potential arising from two equilibria (redox and ion exchange) in the spinel-type manganese oxide. Sensitivity and the influence of pH on the electrode response were directly related to the doping agents present in the oxide structure.

1. Introduction

The attraction of spinel-type manganese oxide is due to the presence of tridimensional tunnels in the crystalline network. These enable topotactic reactions, with the insertion and extraction of lithium ions in the vacancies and interstitial spaces, which permits charge compensation by means of changes in the oxidation state of the manganese ion [1].

$$2Mn^{IV}O_{2(s)} + 2Li^{+}_{(aq)} + H_2O_{(l)} \rightleftharpoons Li_2[Mn_2{}^{(III)}O_4]_{(s)} + 2H^{+}_{(aq)} + \frac{1}{2}O_{2(g)} \quad (1)$$

However, one of the main disadvantages related to the use of this material concerns the decrease in specific capacity during successive charge/discharge cycles, due to the Jahn-Teller effect [1]. This is an anisotropic distortion of the compact cubic symmetry formed by the O^{2-} ions in the spinel $LiMn_2O_4$, resulting in a tetragonal symmetry, and is one of the principal factors hindering use of the material in commercial applications [2,3]. In recent work, study of the partial substitution of manganese ions by other transition metal cations, as well as partial substitution of oxygen ions in manganese oxide by anions, revealed a decrease in the Jahn-Teller effect [4]. Attempts to improve the electrochemical performance of spinel-type manganese oxide have involved doping with divalent or trivalent metals (Ni, Co, Al, Ga, and Cr) to partially substitute the manganese ions in the spinel structure [5–8], or with anions to partially substitute the oxygens [9]. Simultaneous doping with cations and anions has also been investigated [5].

Doping with cations can improve the stability of the manganese oxide structure when the partial substitution is performed using a cation with smaller ionic radius than that of the manganese (0.65 Å) in the spinel structure. Amaral et al. [5] found that the ionic radius of cation dopants such as Al, Co, and Ga (ionic radii of 0.53, 0.60, and 0.63 Å, respectively) directly affected the unit cell parameter of manganese oxide, with values of 8.229, 8.230, and 8.231 Å, respectively, which were smaller than that of the pure spinel material (8.234 Å). In relation to the stability of the oxide, the partial substitution resulted in a decrease in the Mn^{3+}/Mn^{4+} ratio, due to substitution of the Mn^{3+} ions in the structure, which are responsible for the Jahn-Teller distortion [10]. In the case of doping with anions, the effect of the anion on the electrochemical

* Corresponding author.

http://dx.doi.org/10.1016/j.electacta.2015.05.177
0013-4686/

performance of manganese oxide remains unclear. However, it is known that anionic doping reduces the dissolution of manganese in the electrolyte [5], consequently improving the structural stability of the oxide during insertion of the lithium ions [11,12].

Earlier work by our research group studied the effect of aluminum doping on the potentiometric performance of an electrode based on spinel-type manganese oxide for the selective detection of lithium ions [13]. It was found that the performance of the selective electrode was superior to that of non-doped manganese oxide [14], demonstrating that the Al(III) doping increased the structural stability of the material and improved the potentiometric response and sensitivity of the sensor. A super-Nernstian response of the sensor was obtained at pH 10. Similar improvement in electrochemical performance was found by Venugopal et al. [15], who studied the potentiometric response of a modified electrode consisting of spinel-type manganese oxide doped with Cr(III).

The present work describes a comparative study of the influence of anion doping (using S^{2-} and F^{-}) in gallium-substituted spinel manganese oxide on the potentiometric performance of an electrode selective to lithium ions. Evaluation was made of the effect of solution pH, as well as the selectivity towards lithium ions rather than other alkali metal and alkaline-earth metal ions. Investigation of the potentiometric behavior of the oxide provided insights into the sensor response mechanism.

2. Experimental

2.1. Reagents and solutions

All chemicals were analytical reagent grade and were used without further purification. The supporting electrolyte used for all experiments was a 0.1 mol L^{-1} Tris(hydroxymethyl) aminomethane (TRIS) buffer solution (pH = 10). A 0.010 mol L^{-1} lithium ions solution was prepared daily by dissolving LiCl (Merck) in 100 mL of TRIS buffer. For the study of interfering ions NaCl, KCl, RbCl, CsCl, $MgCl_2$, $CaCl_2$, $SrCl_2$ and $BaCl_2$ were dissolved in the TRIS buffer.

2.2. Synthesis and characterization of the anion-doped gallium-substituted manganese oxide spinel

The anion-doped gallium-substituted manganese oxide was prepared and characterized by research group of the Prof. Bocchi [5]. The doped spinels were synthesized from by ε-MnO_2 [16], LiOH (Riedel de Haën), Ga_2O_3 (Aldrich) and Li_2S (Aldrich) or LiF (Aldrich) by solid-state reaction. When $Li_{1.05}Ga_{0.02}Mn_{1.98}O_4$ was the objective, the anionic salts were omitted. The precursors in the mole ratios $1.00(Mn_{1.98} + Ga_{0.02})(O_{1.98} + S_{0.02})$:1.05Li and $1.00(Mn_{1.98} + Ga_{0.02})(O_{1.98} + F_{0.02})$:1.05Li were prepared. After homogenization in a mortar, the precursor mixture was calcined in a tubular oven under static air at 750 °C for 72 h and then slowly cooled at a rate of −10 °C min^{-1}. A mixer mill (Spex Certiprep 8000 M) was used for milling the doped spinels for 30 min [5]. The anion-doped gallium-substituted manganese oxide was characterized by X-ray diffractometry (XRD) using an automated diffractometer (Shimadzu modelo XRD-6000) with Cu Kα radiation (30 kV and 40 mA) and graphite monochromator at a scan rate of 0.02° min^{-1} in an interval at 5° to 50°.

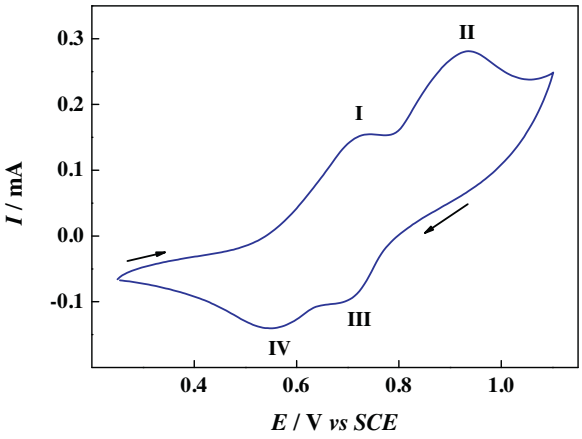

Fig. 1. Typical cyclic voltammogram obtained at 5 mV s^{-1} for CPEM with $Ga_{0.02}Mn_{1.98}O_4$ in 0.10 mol L^{-1} ions Li^+ in Tris buffer containing 0.1 mol L^{-1} in pH 10.

2.3. Preparation of the delithiated anion-doped gallium-substituted manganese oxide spinel

For conversion in delithiated form, the doped spinels $Li_{1.05}Ga_{0.02}Mn_{1.98}O_{3.98}X_{0.02}$ ($X = S^{2-}$ or F^{-}) was treated in an aqueous diluted sulfuric acid solution kept under constant stirring during 45 min. When the pH of this mixture became stable, the solution was decanted and the remaining solid material washed by decantation with deionized water, filtered and dried in air at 90 °C. Treatment of the spinel-type material with aqueous acid was found to result in conversion of the $Li_{1.05}Ga_{0.02}Mn_{1.98}O_{3.98}X_{0.02}$ to nearly pure $Ga_{0.02}Mn_{1.98}O_{3.98}X_{0.02}$, preserving the spinel structural. The manganese oxide has empty tetrahedral sites, and is designated as delithiated spinel and the Li^+ can re-enter in the empty sites of this oxide.

2.4. Selective Electrode Construction

The selective electrodes were prepared by carefully mixing 55% (m/m) of graphite powder (1-2 μm particle size, Aldrich), 25% (m/m) anion-doped gallium-substituted manganese oxide and 20% (m/m) of mineral oil (Aldrich). Those mixtures were prepared by magnetic stirring in Becker (50 mL) containing 20 mL of hexane. The final pastes were obtained by evaporation of the solvent. The modified carbon pastes were packed into an electrode body, consisting of a plastic cylindrical tube (o.d. 7 mm, i.d. 4 mm) equipped with stainless steel staff serving as an external electric contact. Packing paste was achieved by pressing the electrode surface (surface area of 12.6 mm^2) against a filter paper. Before the use, the electrodes were activated by cyclic voltammetry in 0.1 mol L^{-1} TRIS buffer solution (pH 10) containing lithium ions.

2.5. Apparatus

Cyclic voltammetric and potentiometric measurements were carried out with an μ-Autolab type III (Eco Chimie) controlled by a personal computer. All the measurements were performed at a constant temperature (25 °C), in a thermostated electrochemical cell. The cyclic voltammetric measurements were performed in a three-electrode cell using a carbon paste electrode modified (CPEM) with an anion-doped galium-substituted manganese oxide spinel as a working electrode (indicator electrode), saturated calomel electrode (SCE) as reference and platinum auxiliary electrode. The potential range was from 0.25 to 1.10 V (*vs.* SCE) at scan rate of 05 mV s^{-1}, and during the measurements the solution in the cell was not flowed. The potential differences between the working (CPEM) and reference electrodes were measured using the GPES software (Eco Chimie) by chronopotentiometry (zero current).

3. Results and discussion

3.1. Characterization of the $Ga_{02}Mn_{1.98}O_{3.98}X_{0.02}$

X-ray diffractograms of the delithied spinel $Ga_{0.02}Mn_{1.98}O_{3.98}X_{0.02}$ (Supplementary Material I) showed crystallographic

Table 1
Initial potential, potential and time of stabilization of a carbon paste electrode modified for each concentration in the activation process.

Doping	$[Li^+]$ activation (mol L^{-1})	E_i (mV)	E_{stab} (mV)	Stabilization time (s)
Gallium	1.0×10^{-4}	380	346	> 7200
	1.0×10^{-3}	327	307	~ 700
	1.0×10^{-2}	337	305	~ 1600
	0.10	378	302	~ 6800
Gallium and Sulfur	1.0×10^{-4}	403	367	> 7200
	1.0×10^{-3}	317	299	~ 5800
	1.0×10^{-2}	351	293	~ 6600
	0.10	460	285	> 7200
Gallium and Fluor	1.0×10^{-4}	389	370	> 7200
	1.0×10^{-3}	328	324	~ 7000
	1.0×10^{-2}	347	320	> 7200
	0.10	403	317	> 7200

E_i = initial potential; E_{stab} = stabilized potential

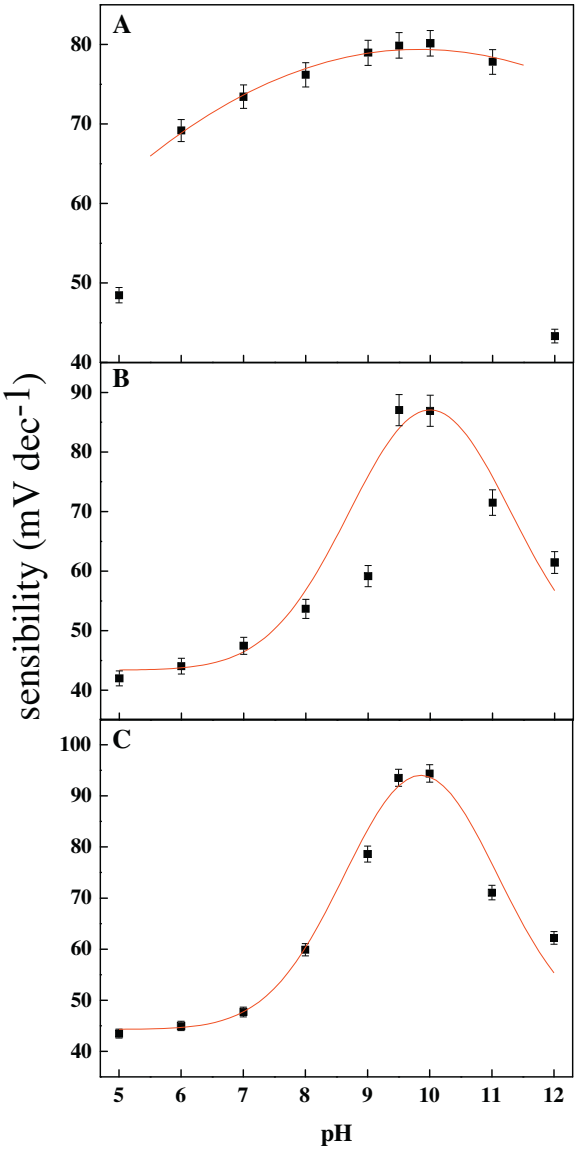

Fig. 2. Effect of pH on the potentiometric response of the spinel type manganese oxide doped: A: $Ga_{0.02}Mn_{1.98}O_4$; B: $Ga_{0.02}Mn_{1.98}S_{0.02}O_{3.98}$; and C: $Ga_{0.02}Mn_{1.98}F_{0.02}O_{3.98}$.

phases in agreement with JCPDS file #89-8325, with cubic phase spinel and the presence of the *Fd3m* spatial group. The analyses also indicated that the doping did not significantly affect the crystalline structure of the oxide. The greatest change observed after anionic doping concerned the unit cell parameter of the manganese oxide. The value of unit cell parameter *a* decreased in the order: $Ga_{0.02}Mn_{1.98}O_4$ (8.231 Å) > $Ga_{0.02}Mn_{1.98}O_{3.98}S_{0.02}$ (8.230 Å) > $Ga_{0.02}Mn_{1.98}O_{3.98}F_{0.02}$ (8.229 Å). It is important to emphasize that this trend was different to those observed for the spinel material doped with different cations [5,7,10], where it was found that the unit cell parameter of the manganese oxide was lower for dopants with smaller ionic radius. However, this was unable to explain the value of the unit cell parameter for the oxide doped with S^{2-}, because the ionic radius of S^{2-} (1.84 Å) is greater than that of O^{2-} (1.40 Å) [17]. In this case, the smaller value of *a* for the oxide doped with sulfur could have been due to the oxidation of S^{2-} during calcination of the reaction mixture, with consequent decrease in the ionic radius. According to Cheng et al. [18], there are two possible structural models for the substitution following anionic doping, either involving insertion of the anion into the interstices of the crystalline structure, or substitution of O^{2-} in the crystalline network by the dopant anions.

3.2. Study electrochemical sensor

The activation of the electrode was studied in order to obtain the best performance of the potentiometric sensor. Activation consisted of the insertion/extraction of lithium ions in the porous oxide matrix using cyclic voltammetry at different scanning speeds. The influence of the concentration of lithium in the electrolyte was evaluated in terms of the subsequent potentiometric response. The voltammograms (Fig. 1) showed two peaks for both potential scanning directions, indicating that the reactions associated with the insertion/extraction of the lithium ions in the oxide occurred in two stages:

$$Li^+_{(aq)} + 2\ MnO_{2(s)} + e^- \rightarrow Li_1Mn_2O_{4(s)}\ (\text{peaks II / III}) \quad (2)$$

$$Li^+_{(aq)} + Li_1Mn_2O_{4(s)} + e^- \rightarrow Li_2Mn_2O_{4(s)}\ (\text{peaks I / IV}) \quad (3)$$

The electrode was activated using different potential scanning rates (5, 10, 25, and 50 mV s^{-1}) and lithium ion concentrations (0.10 to 1.0×10^{-4} mol L^{-1}). The electrolyte solution was Tris buffer at pH 10.0. After each activation, the electrode was transferred to a conventional electrochemical cell containing 0.1 mol L^{-1} Tris buffer kept under constant agitation, in the absence of lithium ions. The chronopotentiometry method (with zero current) was

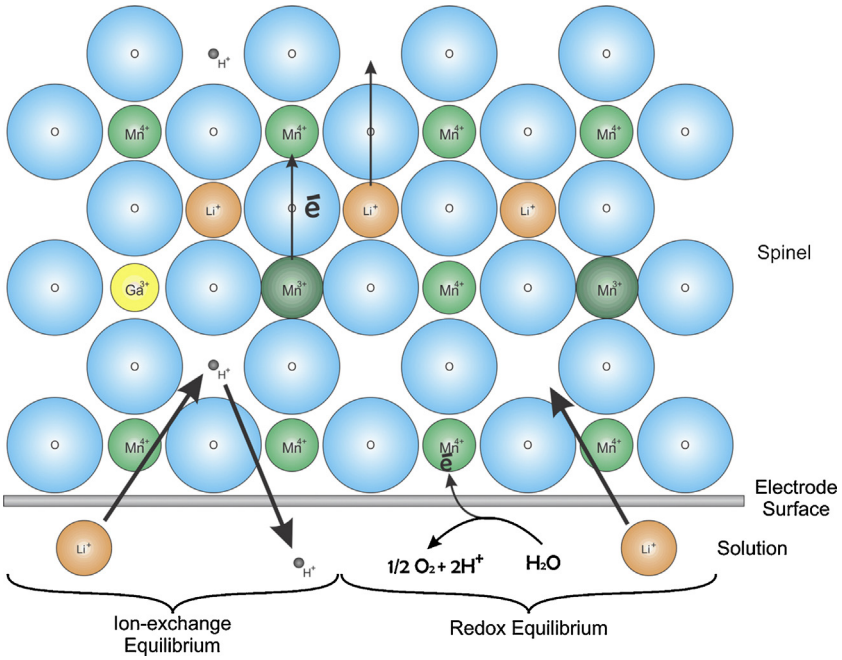

Scheme 1. Representation of the potentiometric response to selective sensor for lithium ions. Representation insertion/extraction of lithium ions. Adapted scheme [24].

Table 2
Sensitivity of the spinel type manganese oxides doped opposite the influence of pH variation.

pH	Sensibility (mV dec^{-1})		
	Ga	GaS	GaF
5	48.5	42.0	43.5
6	69.2	44.1	45.0
7	73.4	47.5	47.7
8	76.2	53.7	60.0
9	79.0	59.2	78.6
9.5	80.0	87.0	93.5
10	80.2	86.9	94.4
11	77.8	71.5	71.1
12	43.0	61.4	62.2

used to determine the stabilization time, the change in potential, and the equilibrium potential of the electrode (Table 1).

Electrode stabilization is related to the equilibrium between the quantities of lithium in the porous matrix and the aqueous phase [10]. During the potential scanning, in the activation step, lithium ions are inserted into the porous oxide matrix from the electrolyte solution. The degree of insertion varies locally during the process, as a function of the concentration of lithium ions in solution. This effect has been observed previously for spinel-type manganese oxide [19,20], and was qualitatively interpreted in terms of the coefficient of diffusion of the ion in the solid state, depending on the predetermined degree of insertion [21]. A greater degree of insertion of lithium ions in the doped manganese oxide matrix considerably reduces the coefficient of diffusion of the ion in the porous matrix, hence altering the stabilization equilibrium at the solid/aqueous interface. It can be seen from the data in Table 1 that use of a higher concentration of lithium ions during electrode activation resulted in a greater degree of insertion into the porous oxide matrix. Consequently, a longer stabilization time was required to achieve equilibrium at the solid/aqueous interface. It can also be seen that there was a significant influence of doping on the stabilization time. The oxide doped only with gallium showed shorter stabilization times for all the concentrations tested, compared to the oxides doped with anions (F^- and S^{2-}). This was directly related to the unit cell size of the oxide, and consequently to diffusion of the lithium ions in the porous matrix. A smaller unit cell size resulted in greater difficulty in insertion/extraction of the lithium ions in the porous structure of the doped oxide. These findings were in agreement with our earlier work that demonstrated the influence of doping on the electrochemical activity of spinel-type manganese oxide [13].

The results of the sensor activation and stabilization experiments indicated that a solution containing lithium ions at a concentration of 1.0×10^{-3} mol L^{-1} was ideal for activation of all the oxides tested in this work.

3.3. Performance evaluation potentiometric

Firstly, evaluation was made of the influence of pH on the potentiometric response of the electrode. An analytical curve was constructed, with electrode potential plotted against log (a_{Li}^+), and the angular coefficient (mV dec^{-1}) was determined for each pH level tested (pH 5-12).

The pH of the electrolyte solution has a direct influence on electrode performance, mainly because it affects the stability of the doped oxide structure and the insertion of H^+ ions into the porous matrix. Fig. 2 shows the influence of pH on the potentiometric sensitivity (mV dec^{-1}) of the electrode. For all the oxides studied, the maximum sensitivity was obtained at a pH of around 9.75 ± 0.25. These optimum pH values were higher than the optimum pH for pure spinel-type manganese oxide (pH ≅ 8) [15].

Between pH 5 and 9, there was a marked decrease in the sensitivity of the selective electrode, which was due to two factors: (1) disproportionation reactions of Mn^{3+} ions present at the manganese oxide matrix surface [14]; and (2) ion exchange reactions between lithium ions in the tunnel and hydrogen ions in the aqueous phase. In recent work, we found that the substitution of a fraction of the manganese ions in the oxide matrix increased the number of ion exchange sites in the solid that were not involved in the extraction/insertion redox reactions (Scheme 1). However, the manganese(III) disproportionation reaction can occur at the surface, regardless of the presence of redox or ion exchange sites. At pH above 10, the sensitivity again decreased,

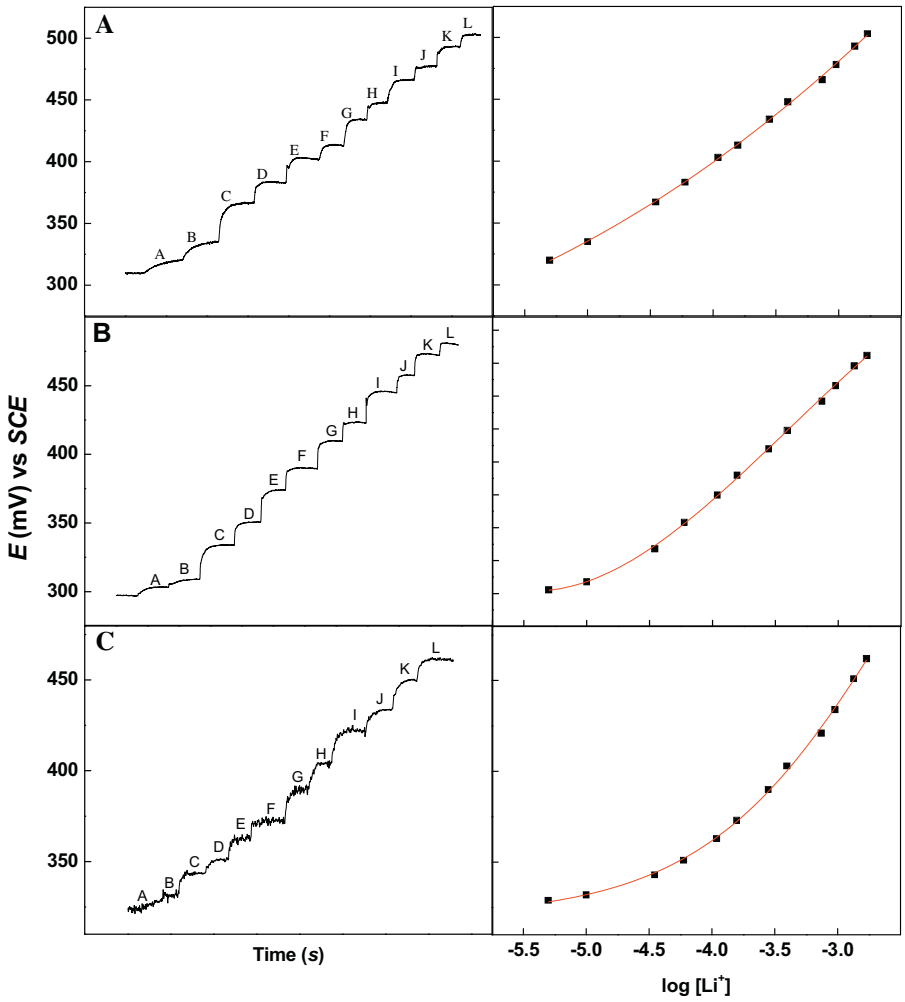

Fig. 3. Potentiometric response of doped sensor: A: $Ga_{0.02}Mn_{1.98}O_4$; B: $Ga_{0.02}Mn_{1.98}S_{0.02}O_{3.98}$; and C: $Ga_{0.02}Mn_{1.98}F_{0.02}O_{3.98}$ in different concentrations of Li^+. A) 4.99×10^{-6}; B) 9.99×10^{-6}; C) 3.49×10^{-5}; D) 5.96×10^{-5}; E) 1.09×10^{-4}; F) 1.57×10^{-4}; G) 2.77×10^{-4}; H) 3.94×10^{-4}; I) 6.19×10^{-4}; J) 8.34×10^{-4}; K) 1.23×10^{-3} and L) 1.62×10^{-3} mol L^{-1}.

Table 3
Detection limit, linear range and sensitivity of the modified electrodes.

Doping	Detection Limit (mol L^{-1})	Linear Range (mol L^{-1})	Sensibility (mV dec^{-1})	R
Ga	1.09×10^{-5}	3.49×10^{-5} - 1.62×10^{-3}	80.2	0.998
GaS	1.62×10^{-5}	5.96×10^{-5} - 1.62×10^{-3}	87.0	0.999
GaF	3.16×10^{-5}	2.77×10^{-4} - 1.62×10^{-3}	94.4	0.991

probably due to the gradual formation of a poorly ordered surface layer that acted to block the diffusion of lithium ions. Gu et al. [22] studied the mechanism of proton-induced cathode dysfunction in lithium ion batteries and found that the electrochemical stability of the cathode in an aqueous lithium salt electrolyte was critically dependent on the pH of the solution.

Of the oxides studied, $Ga_{0.02}Mn_{1.98}O_4$ showed the lowest influence of pH on the potentiometric response (Table 2), clearly indicating that doping with gallium helped to minimize the interfacial effects in the manganese disproportionation reaction. This was not evident in the case of the $Ga_{0.02}Mn_{1.98}O_{3.98}S_{0.02}$ and $Ga_{0.02}Mn_{1.98}O_{3.98}F_{0.02}$ oxides, despite the presence of gallium ions in their compositions. It is likely that anion substitution in the oxide was related to the formation of ion exchange sites in the solid, and that the insertion equilibrium was strongly influenced by the hydrogen ion concentration.

Using the ideal pH in TRIS buffer, the electrodes as potentiometric sensors for lithium was evaluated by concentration ranging from 4.99×10^{-6} to 1.62×10^{-3} mol L^{-1} of lithium ions in solution. The zero current chronopotentiometric responses (Fig. 3) were obtained by the progressive additions of lithium in 0.1 mol L^{-1} TRIS solution under continuous stirring at 300 rpm. The potentials for the different concentrations of lithium ion were recorded in order to obtain the typical analytical curves. In general, the electrode response time was fast for the different lithium concentrations, presenting stable potential in ± 250 seconds.

Table 3 presents the analytical performance of the electrodes in terms of linear range, detection limit, and sensitivity, from which it can be seen that doping had direct effects on these parameters. The linear ranges of the potentiometric responses of the sensors followed the increasing order: $Ga_{0.02}Mn_{1.98}O_4 > Ga_{0.02}Mn_{1.98}O_{3.98}S_{0.02} > Ga_{0.02}Mn_{1.98}O_{3.98}F_{0.02}$. The detection limits decreased in the order: $Ga_{0.02}Mn_{1.98}O_4 < Ga_{0.02}Mn_{1.98}O_{3.98}S_{0.02}$

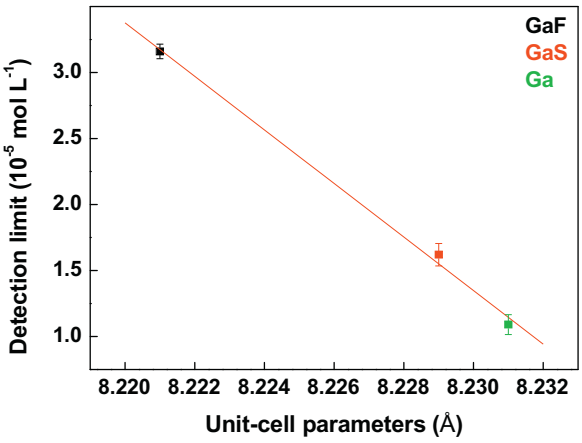

Fig. 4. Detection limit *versus* unit-cell parameter for each doped oxide.

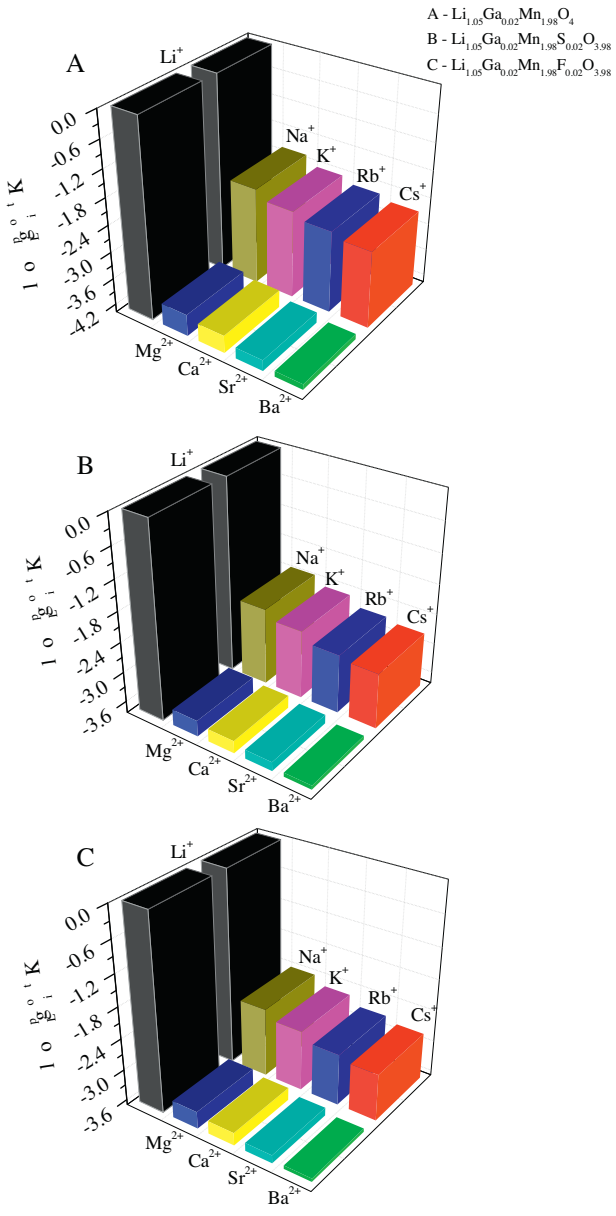

Fig. 5. Logarithm of the potentiometric selectivity coefficients ($\log K^{pot}_{Li,X}$) oxide: A: $Ga_{0,02}Mn_{1,98}O_4$; B: $Ga_{0,02}Mn_{1,98}S_{0,02}O_{3,98}$; and C: $Ga_{0,02}Mn_{1,98}F_{0,02}O_{3,98}$.

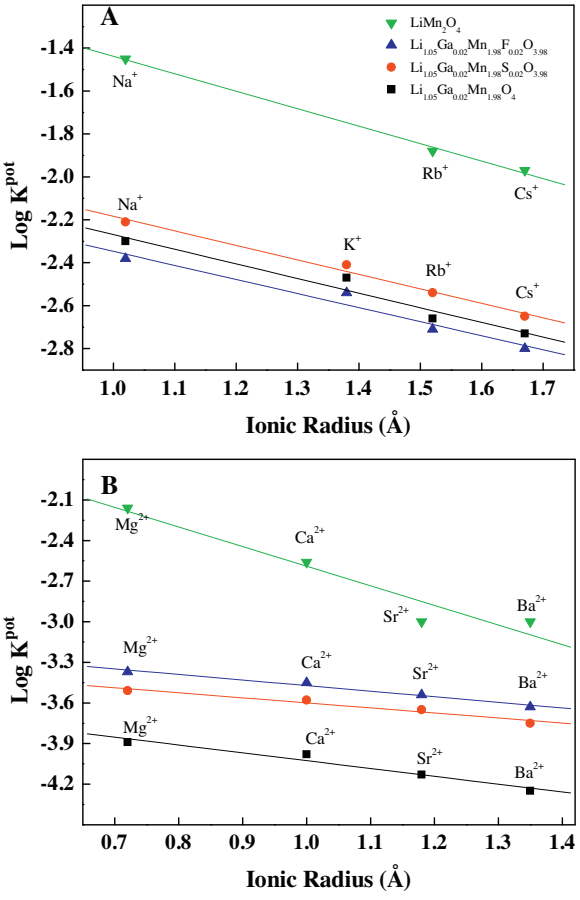

Fig. 6. Logarithm of the potentiometric selectivity coefficient ($\log K^{pot}_{Li,X}$) versus ionic radius (IR) to: A: alkali metals and B: alkaline earth metals.

$< Ga_{0.02}Mn_{1.98}O_{3.98}F_{0.02}$. Interestingly, there was a relationship between the detection limit of the electrode and the unit cell size (see Fig. 4), which could be explained by the effect of doping on the crystalline unit cell parameter, and consequently on the pore size of the oxide matrix. A decrease in the size of the insertion tunnel affected the rate of diffusion of the lithium ions in the crystalline structure. Computational studies of spinel structure $LiMn_2O_4$ [23] indicate that activation energy for ion transport in the oxide structure is in function of the distance between the oxygen layers on each side of the Li plane. The decrease of the activation energy is related with the increase of the space between the oxygen layers.

In the evaluation of the potentiometric selectivity of the sensors was studied by fixed interferent method [24]. For this, the potentiometric measurements were carried out by varying the lithium concentration as above, but in this case in the presence of a fixed interfering ion concentration (1.0×10^{-2} mol L^{-1}). The selectivity coefficient was estimated according to Eq. (5):

$$K^{pot}_{LiX} = a_{Li}/a_X z_{Li}/z_X \quad (5)$$

Where a_{Li} is activity of the lithium ions in solution, a_X is activity of the interferent ion, Z_{Li} is charge of the lithium ion and Z_X is the charge of the interferent ion. Fig. 5 presents the values of the logarithm of potentiometric selectivity coefficient ($\log K^{pot}_{Li,X}$) for each studied electrode. The selectivity of the doped spinel is related the lattice and structural parameters. Increased potentiometric selectivity of the sensor was associated with decreases in the unit cell parameter of the doped oxide and the size of the tridimensional tunnels housing the lithium ions in the crystalline structure (Supplementary Material II). As explained above, the

shrinkage of the channel exerts an increase in the activation energy of insertion into the porous oxide matrix. The selectivity of the sensor was better compared to electrode based in the undoped spinel-type manganese oxide [14].

There was a direct relation between the selectivity of the doped spinel-type sensor and the ionic radius of the dopant cation (Fig. 6). The potentiometric selectivity of sensor decrease linearly with increase ionic radius of the alkaline-metal ions ($Na^+ > K^+ > Rb^+ > Cs^+$). The same behavior is observed for earth-alkaline metal ions ($Mg^{2+} > Ca^{2+} > Sr^{2+} > Ba^{2+}$), but the amplitude were lower than alkaline ions. As already noted, charge density, ionic size and the lattice spacing on the surface of manganese oxide are important factors in the insertion phenomenon [13,14]. The observed difference may be assigned to higher energies for dehydration which is needed for uptake of ion into the crystal structure from the solution. The degree of selectivity of the sensor ($Ga_{0,02}Mn_{1,98}O_{3,98}F_{0,02} > Ga_{0,02}Mn_{1,98}O_{3,98}S_{0,02} > Ga_{0,02}Mn_{1,98}O_4$) follows the order of size oxide unit cell.

4. Conclusion

In conclusion, we have investigated the influence of the gallium and anions in the spinel-type manganese oxide on the performance of potentiometric sensors for lithium ion in aqueous solutions. The most relevant observation was the influence of the unit cell volume about the linear interval response, detection limit and selectivity of the sensor The sensitivity and the influence of pH on electrode response is related exclusively with doping element in the oxide structure.

Acknowledgments

The authors gratefully acknowledge the Brazilian-funding agencies CNPq (474367/2004-5) and FAPESP (2005/01296-4) financial support for this work.

Appendix A. Supplementary data

Supplementary data associated with this article can be found, in the online version, at http://dx.doi.org/10.1016/j.electacta.2015.05.177.

References

[1] K. Miyazaki, C.N. Xu, M. Hieda, New Potential-Type Humidity Sensor Using Emd-Based Manganese Oxides as a Solid-Electrolyte, Journal of the Electrochemical Society 141 (1994) L35–L37.
[2] K. Miura, A. Yamada, M. Tanaka, Electric states of spinel $Li_xMn_2O_4$ as a cathode of the rechargeable battery, Electrochimica Acta 41 (1996) 249–256.
[3] D. Guyomard, J.M. Tarascon, Carbon $Li_{1+x}Mn_2O_4$ System, Solid State Ionics 69 (1994) 222–237.
[4] A. Yamada, Lattice instability in $Li(Li_xMn_{2-x})O_4$, Journal of Solid State Chemistry 122 (1996) 160–165.
[5] F.A. Amaral, N. Bocchi, R.F. Brocenschi, S.R. Biaggio, R.C. Rocha, Structural and electrochemical properties of the doped spinels $Li_{1.05}M_{0.02}Mn_{1.98}O_{3.98}N_{0.02}$ ($M = Ga^{3+}$, Al^{3+}, or Co^{3+}; $N = S^{2-}$ or F^-) for use as cathode material in lithium batteries, Journal of Power Sources 195 (2010) 3293–3299.
[6] S.R. Das, S.B. Majumder, R.S. Katiyar, Kinetic analysis of the Li^+ ion intercalation behavior of solution derived nano-crystalline lithium manganate thin films, Journal of Power Sources 139 (2005) 261–268.
[7] P. Lucas, C.A. Angell, Synthesis and diagnostic electrochemistry of nanocrystalline $Li_{1+x}Mn_{2-x}O_4$ powders of controlled Li content, Journal of the Electrochemical Society 147 (2000) 4459–4463.
[8] J.M. Amarilla, J.L.M. de Vidales, R.M. Rojas, Electrochemical characteristics of cobalt-doped $LiCo_yMn_{2-y}O_4$ ($0 \le y \le 0.66$) spinels synthesized at low temperature from $Co_xMn_{3-x}O_4$ precursors, Solid State Ionics 127 (2000) 73–81.
[9] H.R. Lee, B. Lee, K.Y. Chung, B.W. Cho, K.Y. Lee, S.H. Oh, Scalable synthesis and electrochemical investigations of fluorine-doped lithium manganese spinel oxide, Electrochimica Acta 136 (2014) 396–403.
[10] J.H. Lee, J.K. Hong, D.H. Jang, Y.K. Sun, S.M. Oh, Degradation mechanisms in doped spinels of $LiM_{(0.05)}Mn_{(1.95)}O_{(4)}$ (M = Li, B, Al, Co, and Ni) for Li secondary batteries, Journal of Power Sources 89 (2000) 7–14.
[11] K.Y. Chung, C.W. Ryu, K.B. Kim, Onset mechanism of Jahn-Teller distortion in 4 V $LiMn_2O_4$ and its suppression by $LiM_{0.05}Mn_{1.95}O_4$ (M = Co, Ni) coating, Journal of the Electrochemical Society 152 (2005) A791–A795.
[12] M. Wakihara, Lithium manganese oxides with spinel structure and their cathode properties for lithium ion battery, Electrochemistry 73 (2005) 328–335.
[13] B.H. Freitas, F.A. Amaral, N. Bocchi, M.F.S. Teixeira, Study of the potentiometric response of the doped spinel $Li_{1.05}Al_{0.02}Mn_{1.98}O_4$ for the optimization of a selective lithium ion sensor, Electrochimica Acta 55 (2010) 5659–5664.
[14] M.F.S. Teixeira, E.T.G. Cavalheiro, M.F. Bergamini, F.C. Moraes, N. Bocchi, Use of a carbon paste electrode modified with spinel-type manganese oxide as a potentiometric sensor for lithium ions in flow injection analysis, Electroanalysis 16 (2004) 633–639.
[15] N. Venugopal, B.C. Yang, H. Yoon, K.S. Chung, B.G. Kim, T. Ko, Graphite based electrode modified with delithiated spinel $Li_{1.0}Cr_{0.05}Mn_{1.95}O_4$ for Li ion selective sensor, Material Research Innovations 15 (2011) 324–329.
[16] E.A. Laurindo, F.A. Amaral, M.L. dos Santos, L.C. Ferracin, A. Carubelli, N. Bocchi, R.C. Rocha, Production of electrolytic manganese dioxide for usage in lithium batteries, Quimica Nova 22 (1999) 600–604.
[17] L.H. Ahrens, Ionic Radii of the Elements, American Mineralogist 37 (1952) 283–283.
[18] H. Cheng, K. Scott, Carbon-supported manganese oxide nanocatalysts for rechargeable lithium-air batteries, Journal of Power Sources 195 (2010) 1370–1374.
[19] T. Kashiwagi, M. Nakayama, K. Watanabe, M. Wakihara, Y. Kobayashi, H. Miyashiro, Relationship between the electrochemical behavior and Li arrangement in $Li_xM_yMn_{2-y}O_4$ (M = Co, Cr) with spinel structure, Journal of Physical Chemistry B 110 (2006) 4998–5004.
[20] R. Thirunakaran, A. Sivashanmugam, S. Gopukumar, C.W. Dunnill, D.H. Gregory, Studies on chromium/aluminium-doped manganese spinel as cathode materials for lithium-ion batteries: A novel chelated sol-gel synthesis, Journal of Materials Processing Technology 208 (2008) 520–531.
[21] G.G. Amatucci, N. Pereira, T. Zheng, I. Plitz, J.M. Tarascon, Enhancement of the electrochemical properties of $Li_1Mn_2O_4$ through chemical substitution, Journal of Power Sources 81 (1999) 39–43.
[22] V.H. Nguyen, H.B. Gu, $LiFePO_4$ batteries with enhanced lithium-ion-diffusion ability due to graphene addition, Journal of Applied Electrochemistry 44 (2014) 1153–1163.
[23] A.D. Roberts, X. Li, H.F. Zhang, Porous carbon spheres and monoliths: morphology control, pore size tuning and their applications as Li-ion battery anode materials, Chemical Society Review 43 (2014) 4341–4356.
[24] Y. Umezawa, P. Buhlmann, K. Umezawa, K. Tohda, S. Amemiya, Potentiometric selectivity coefficients of ion-selective electrodes Part I. Inorganic cations, Pure and Applied Chemistry 72 (2000) 1851–2082.